Published in final edited form as:
J Neurochem. 2006 April ; 97(1): 44–56. doi:10.1111/j.1471-4159.2006.03701.x.

Matrix metalloproteinase-7 disrupts dendritic spines in hippocampal neurons through NMDA receptor activation

Tina V. Bilousova[*], **Dmitri A. Rusakov**[†], **Douglas W. Ethell**[*], and **Iryna M. Ethell**[*]

[*]Division of Biomedical Sciences, University of California Riverside, California, USA

[†]Institute of Neurology, University College London, London, UK

Abstract

Dendritic spines are protrusions from the dendritic shaft that host most excitatory synapses in the brain. Although they first emerge during neuronal maturation, dendritic spines remain plastic through adulthood, and recent advances in the molecular mechanisms governing spine morphology have shown them to be exquisitely sensitive to changes in the micro-environment. Among the many factors affecting spine morphology are components and regulators of the extracellular matrix (ECM). Modification of the ECM is critical to the repair of injuries throughout the body, including the CNS. Matrix metalloproteinase (MMP)-7/matrilysin is a key regulator of the ECM during pathogen infection, after nerve crush and in encephalitogenic disorders. We have investigated the effects of MMP-7 on dendritic spines in hippocampal neuron cultures and found that it induces the transformation of mature, short mushroom-shaped spines into long, thin filopodia reminiscent of immature spines. These changes were accompanied by a dramatic redistribution of F-actin from spine heads into thick, rope-like structures in the dendritic shaft. Strikingly, MMP-7 effects on dendritic spines were similar to those of NMDA treatment, and both could be blocked by channel-specific antagonists. These findings are the first direct evidence that MMPs can influence the morphology of mature dendritic spines, and hence synaptic stability.

Keywords

actin cytoskeleton; dendritic spine; hippocampal neuron; matrilysin; metalloproteinase; NMDA receptor

Dendritic spines are the most common postsynaptic sites for excitatory synapses within the CNS. Alterations in the number and morphology of spines play a critical role in regulating the synaptic development and plasticity that underlie learning and memory (Yuste and Bonhoeffer 2001). Abnormal spine development has been implicated in an array of cognitive disorders associated with mental retardation and autism, as well as neurodegeneration (Kaufmann and Moser *et al.* 2000; Fiala *et al.* 2002; Ramakers 2002). The formation and stability of spines can be affected by a wide variety of stimuli, such as learning paradigms, hormonal regulation, molecular interactions and ion channel activity (Yuste and Bonhoeffer 2001; Hering and Sheng 2001; Nimchinsky *et al.* 2002). This sensitivity to changes in the local micro-environment makes spines especially susceptible to

Address correspondence and reprint requests to Iryna Ethell or Doug Ethell, Biomedical Sciences, University of California, Riverside, CA 92521–0121, USA. iryna.ethell@ucr.edu or doug.ethell@ucr.edu.

Supplementary Material The following material is available for this paper online.
This material is avaialble as part of the online article from http://www.blackwell-synergy.com

Europe PMC Funders Author Manuscripts

pathological disturbances. For example, a major pathological feature of Alzheimer's disease is an early loss of synapses within the pyramidal layer of hippocampus, thought to result from the synaptotoxicity of soluble β-amyloid (Kayed *et al.* 2003; Cleary *et al.* 2005).

A network of *trans*-synaptic communications, interactions with surrounding astrocytes, the extracellular matrix (ECM) and other external stimuli are integrated as changes in spine properties (Ethell and Pasquale 2005). Elements of the ECM surround dendritic spines and extend into synapses, such that changes in ECM composition can significantly affect synaptic plasticity (Dityatev and Schachner 2003). Integrins and proteoglycans are involved in ECM effects on synaptic strength, but the mechanisms involved in the structural plasticity of spines remain unresolved.

The family of aptly named matrix metalloproteinases (MMPs) can collectively cleave all ECM components in addition to a number of cell surface proteins, which can have profound effects on cell behavior (Mott and Werb 2004). The MMP family is currently comprised of 28 mostly secreted proteins, although new membrane-type MMPs (MT-MMPs) members are still being discovered. MMPs are produced as proforms that require proteolytic cleavage to remove a cysteine switch from the catalytic domain and achieve full activity. The direct cleavage of ECM proteins by MMPs can change binding preferences and affinities; for example MMP cleavage of laminin-5 generates a γ2 fragment, exposing an otherwise inaccessible RGD site that can induce epithelial cell motility (Giannelli *et al.* 1997; Pirila *et al.* 2003). MMP cleavage can also release factors sequestered in the ECM, such as transforming growth factor-β and fibroblast growth factor that have their own potent activities (Imai *et al.* 1997). Further, MMP shedding of membrane protein fragments can affect cell signaling: such as the 80-kDa cleavage product of E-cadherin that induces cell invasion into type I collagen (Lochter *et al.* 1997; Noe *et al.* 2001), the cleavage of the membrane-bound TNF-α that converts it into a soluble pleiotrophic cytokine (Wilson and Matrisian 1996), or cleavage of the apoptosis initiator Fas ligand (FasL) that abrogates high order surface clustering and cell death activity (Mitsiades *et al.* 2001; Ethell and Buhler 2003). As MMP cleavage of ECM, membrane and pericellular proteins can result in complex changes to synaptic homeostasis and signaling, MMPs are likely to also play a role in synaptic development and remodeling.

Under normal physiological conditions, only a few MMPs are expressed within the CNS (Hughes *et al.* 2002). However, during pathological disturbances the expression of several MMPs is initiated or increased (Yong *et al.* 2001), the most notable of which is MMP-7/ Matrilysin/PUMP-1. Although not normally found within the CNS, MMP-7 is present at sites of tissue repair, remodeling and pathology throughout the body. MMP-7 expression has been reported in the macrophages of atherosclerotic plaques (Furman *et al.* 2004), in glial cells after optic and sciatic nerve crush (Hughes *et al.* 2002), in Paneth cells of pathogen-infected gut (Lopez-Boado *et al.* 2000), and in arthritic joints (Gjertsson *et al.* 2005), as well as brain and spinal cord extracts from experimental autoimmune encephalomyelitis-induced mice (Anthony *et al.* 1997; Clements *et al.* 1997; Hartung and Kieseier 2000). We have previously reported that MMP-7 can protect cerebellar granular neurons from β-amyloid neurotoxicity, while inducing morphological changes (Ethell *et al.* 2002). Moreover, several known MMP-7 substrates have been implicated in neuronal survival and synaptogenesis, including laminin, collagen, E-cadherin, brevican, TNF-α, heparin-binding EGF, and Fas ligand (reviewed by Woessner 2004).

Given these previous findings, we propose that MMP-7 may play a significant role in the remodeling of excitatory synapses after brain injuries and in neurological disease. We have investigated MMP-7 effects on dendritic spine and synapse morphology in cultured hippocampal neurons. This report provides the first evidence that the stability of dendritic

spines can be disrupted by MMP-7, resulting in dramatic changes in dendritic spine morphology and actin cytoskeletal organization. MMP-7 rapidly and reversibly transformed mature mushroom-like dendritic spines to an immature filopodial morphology without dendritic pruning. We found that the morphological changes induced by MMP-7 are mediated by NMDA receptor (NMDA-R) activation and are completely blocked by the specific antagonist MK-801. These observations may underlie an important mechanism for synaptic remodeling subsequent to injuries, or pathologies that damage the blood–brain barrier and involve MMP-7 expression within the brain.

Experimental procedures

Materials

Recombinant human matrix metalloproteinase-7 (MMP-7/matrilysin; CC1059) was purchased from Chemicon (Temecula, CA, USA). MK-801 (M-107) and *N*-methyl-D-aspartate, NMDA (M-102) were from Research Biochemicals Inc. (Natick, MA, USA). Rhodaminephalloidin (R-416) and Alexa Fluor 488 donkey anti-mouse IgG (A-21202) were obtained from Molecular Probes (Eugene, OR, USA). Monoclonal anti-synaptophysin mouse antibody (clone SVP-38) was from Sigma (St Louis, MO, USA). Neurobasal media 21103, B-27 supplement (17504) and Hank's balanced salt solution (14175) were from Invitrogen (Grand Island, NY, USA). Laminin (354232) and fibronectin (356008) were purchased from BD Biosciences (Bedford, MA, USA). Poly-DL-ornithine (P-8638), L-glutamine (G-3126), bovine serum albumin (9048-46-8), D-(+)-glucose (G-7528), papain (P-4762), deoxyribonuclease-1 (DNase) (D-5025) were obtained from Sigma.

Hippocampal neuron cultures and transfection

Primary cultures of hippocampal neurons were prepared from E15-16 mouse embryos as previously described (Ethell *et al.* 2001), with modifications. Briefly, after treatment with papain (0.5 μg/mL) and Dnase (0.6 μg/mL) for 20 min at 37°C, and mechanical dissociation, E15-16 mouse hippocampal cells were plated on coverslips pre-coated with poly-DL-ornithine (0.5 mg/mL in borate buffer), and laminin [5 μg/mL in phosphate-buffered saline (PBS)] or fibronectin (5 μg/mL in PBS). Cells were maintained in Neurobasal medium supplemented with B27 (Invitrogen), 25 μM glutamate, and 1% penicillin-streptomycin, in a humidified 5% CO_2/10% O_2 incubator at 37°C for 14–17 days. Some hippocampal cultures were transiently transfected with green fluorescent protein (GFP) at 1–5 days *in vitro* (DIV) using a calcium phosphate method as previously described (Ethell *et al.* 2001).

MMP and NMDA treatment

Hippocampal neurons were grown on coverslips for 15 DIV and treated with recombinant human MMP-7 (Chemicon) at concentrations of 0.1–100 mU/mL in conditioned medium. The treatments were performed at 5% CO_2/10% O_2, 37°C for 10 min to 1 h. Treatments with 50 μM NMDA (M-102; Research Biochemicals Inc.) were performed in Hank's balanced salt solution (Invitrogen), containing 1.8 mM $CaCl_2$ without Mg^{2+}. For experiments involving NMDA-R blockade, cultures were pretreated with 10 μM MK-801 (M-107, Research Biochemicals Inc.) in conditioned medium for 2 h; MK-801 was also included in treatment conditions for those experiments.

Fluorescent immunostaining

Neurons grown on glass coverslips were fixed in 4% paraformaldehyde (in PBS), permeabilized with 0.1% Triton X-100 in PBS, and blocked in 5% normal goat serum and 1% bovine serum albumin. Fixed cells were incubated with rhodamine-coupled phalloidin

(1 : 40; R-416; Molecular Probes) and primary mouse anti-synaptophysin (61 μg/mL; clone SVP-38; Sigma); mouse anti-PSD-95 (33 μg/mL, clone 6G6; Affinity BioReagents, Deerfield, IL, USA); mouse anti-MAP2 (5 μg/mL, clone HM-2; Sigma) or mouse anti-neurofilament 200 (4.4 μg/mL, clone NE14; Sigma) antibodies overnight at 4°C. After rinsing three times with PBST (0.05% Tween-20), cells were incubated with Alexa 488-conjugated donkey anti-mouse IgG secondary (4 μg/mL, Molecular Probes). Coverslips were rinsed with PBS and mounted on glass slides with Vectashield (Vector Laboratories, Burlingame, CA, USA). Confocal microscopy was performed using a Zeiss LSM510 confocal microscope (Carl Zeiss Microlmaging Inc.) with a 63 × water immersion objective (numerical aperture 1.2) and 1 × zoom. The Alexa Fluor 488 and rhodamine fluorescent signals were captured using sequential line scanning with double excitation of 488-nm line from an argon laser and 543-nm line from a helium-neon laser. The GFP fluorescence signals were captured using a 488-nm excitation line from an argon laser and LP560 detector. Confocal pinhole was set to one Airey unit. The same photomultiplier tube settings were used for both control and experimental samples, with the most intense fluorescence set just below detector saturation and the background signal set just above the detection floor. Digital images of 1024 × 1024 pixels were collected and imported into Photoshop 7.0.

Live imaging

We monitored the morphology of dendritic spines in 14-DIV GFP-expressing neurons before and after application of MMP-7. Time-lapse imaging was performed under an inverted fluorescence microscope (model TE2000; Nikon) with a 40 × air Fluor objective and monitored by a 12-bit CCD camera (model ORCA-AG; Hamamatsu, Hamamatsu City, Japan) using Image-Pro Plus Software (Media Cybernetics, Silver Spring, MD, USA). The cultures were maintained in neurobasal medium supplemented with B27 at 37°C and 5% CO_2 during the experiment. Images were captured before (0 min) and after (50 min) MMP-7 application.

Image analysis

The effects of MMP-7 on dendritic morphology were examined in 15-DIV GFP-expressing hippocampal neurons as previously described (Ethell and Yamaguchi 1999). Briefly, experimental and control samples were encoded for blind analysis. Note that non-spiny neurons (~20%) were excluded from the analysis. The proximal dendrites (processes extending from the neuronal cell body, at least 1 μm in diameter) were selected for analysis of the length and number of dendritic protrusions. Hidden protrusions that protruded toward the back or front of the viewing plane were not counted. GFP-expressing neurons (10–15) were randomly selected for each experimental group, and three to five proximal dendrites from each neuron were analyzed (~2000 μm of total dendritic length per group). The length of protrusion was determined by measuring the distance between its tip and the base using Image-Pro Plus software. Statistical analysis was performed using Microsoft Excel. Statistical differences between untreated (0 min) and MMP-7-treated (50 min) experimental groups of dendritic protrusions were compared by Student's *t*-test.

Quantitative analyses of the F-actin puncta detected by rhodamine-coupled phalloidin, synaptophysin–immunoreactive puncta, and the sites of their co-localization (overlapping or located in close proximity) were performed as previously described with modifications (Halpain *et al.* 1998). Briefly, experimental and control samples were encoded for blind analysis. The neurons were randomly selected and images were taken using a Zeiss LSM510 confocal microscope (Carl Zeiss Microlmaging Inc.) as described above. Actin clusters (0.5–2 μm in diameter) along dendrites were manually counted using Scion Image software. Those actin clusters that were also positive for synaptophysin (actin/synaptophysin) were scored as spiny synapses. Ten neurons were used in each experimental group, with three to

five dendrites analyzed per neuron. Three independent experiments were performed for each condition. Statistical analysis was performed with unpaired student's *t*-test.

Neuronal apoptosis was determined by analysis of 4′-6-diamidino-2-phenylindole-labeled nuclei as previously described (Ethell *et al.* 2002). Briefly, the coverslips were mounted in 4′-6-diamidino-2-phenylindole-containing mounting medium (Vector Laboratories: H-1200). Experimental and control samples were encoded for blind analysis. Ten random images were collected for each group using an inverted fluorescence microscope (TE2000; Nikon) with a 20 × air Fluor objective. Neuronal survival was calculated as a ratio of the nuclei without apoptotic morphology to the total number of nuclei in each image.

Determining the degree of actin clustering

We carried out the analysis in original (unprocessed and unfiltered) fluorescence images obtained in individual preparations. Dendritic fragments 30–50-μm long were selected arbitrarily (see example in Fig. 3a) and the average pixel brightness across the entire dendritic width was plotted against the distance along the dendrite (see example in Fig. 3b which corresponds to Fig. 3a) using ImageTool (University of Texas Health Science Center San Antonio, San Antonio, TX, USA). The intensity graph thus represented the sampled labeling pattern of actin. To dissect clustering features in such patterns, we followed the stochastic geometry principles described earlier for synaptic scatters in the hippocampus (Rusakov *et al.* 1999). Because the one-dimensional pattern of fluorescence labeling along the dendrite can be thought of as a time series, we could apply a standard autocorrelation function (ACF) analysis to the labeling intensity graphs (Fig. 3). In this case, the ACF values will indicate correlation between the labeling intensities at a chosen interval, termed lag distance, along the dendritic profile. Then, according to the basics of statistics, (i) the height and width of an initial ACF deflection will reflect the occurrence and size of clusters, respectively, (ii) an insignificant deviation of ACF from zero will correspond to the random noise labeling, and (iii) the ACF values close to unity will indicate homogeneous labeling.

In each set of experiments, we analyzed five photographed preparations (5–15 dendritic fragments in each) and obtained the resulting ACF as the average of the five corresponding ACFs. The average ACFs from different experiments were compared on the basis of the corresponding 95% confidence limits. The significance of clustering in the average ACF was assessed using the white noise (zero ACF) standard errors.

Results

MMP-7 induces F-actin rearrangements and reduces spiny synapses

In the early stages of spine development, 7 DIV hippocampal neurons extend many motile thin filopodia, which are driven by linear organized filamentous actin (F-actin) appearing as hair-like extensions along the dendrite, while most F-actin is found within the dendritic shaft. As hippocampal neurons mature, F-actin becomes highly concentrated in spine heads forming highly branched stable structures, which appear as intense puncta along the dendrite with rhodamine-coupled phalloidin staining. To determine the effects of MMP-7 on the dendritic spines in cultured hippocampal neurons, we examined changes in F-actin organization using rhodamine-coupled phalloidin. At 15 DIV, most hippocampal neurons showed F-actin puncta along MAP2-labeled dendrites, but not NF200-labeled axons (Figs 1a and c). Treatment of 15-DIV cultures with recombinant MMP-7 (10 mU/mL) for 1 h induced striking rearrangements of F-actin, including a decrease in F-actin puncta and the appearance of a more homogeneous F-actin staining within the MAP2-labeled dendritic shaft, but not axon (Figs 1b and d).

To observe whether the MMP-7 effects on actin organization in dendrites also affected dendritic spines and spiny synapses, we visualized adjacent presynaptic terminals with immunostaining for synaptophysin (Figs 2a and b) and postsynaptic sites with immunostaining for PSD-95 (Figs 2c and d). Quantitative analysis showed significant reductions in the overall number of F-actin clusters ($p< 0.001$) and number of PSD-95-positive puncta ($p< 0.01$; Fig. 2f) with no significant decreases in the numbers of presynaptic boutons, identified as synaptophysin-positive puncta (Fig. 2e). While the overall number of synaptophysin-positive puncta did not change, their localization was remarkably altered. In control neurons, around 50% of synaptophysin-positive clusters were observed at a distance from the dendritic shaft and were often co-localized with F-actin clusters; this indicated a predominance of spiny synapses (Fig. 2a). In contrast, most synapses in neurons treated with MMP-7 occurred directly on the dendritic shaft (Fig. 2b) and MMP-7 treatment caused a significant reduction ($p< 0.001$) in the number of F-actin and synaptophysin double-positive puncta (Fig. 2e). Autocorrelation function analysis (Figs 3a–d) quantitatively confirmed that the MMP-7 treatment changed F-actin puncta (~2 μm clusters), seen in control dendrites, into a more homogeneous staining pattern (Fig. 3e). Taken together, these findings demonstrate that MMP-7 treatment induces F-actin reorganization within dendrites and reduces the number of spiny synapses in a subset of hippocampal neurons.

MMP-7 induces changes in dendritic spine morphology

To determine whether MMP-7-induced changes in F-actin polymerization in dendritic spines would also affect dendritic spine morphology, we examined the morphology of GFP-labeled dendritic spines before (0 min) and after MMP-7 treatment (50 min). Treatment of 15-DIV hippocampal neurons with MMP-7 induced the elongation of existing spines (Fig. 4e). MMP-7 treatment also altered dendritic spine morphology, transforming dendritic spines with a mushroom-like morphology into filopodia-like thin protrusions (Figs 4a–d). These changes were driven by F-actin reorganization from mesh-like structures in dendritic spine heads into linear organized F-actin in dendritic filopodia (Fig. 3d)

MMP-7 effects are time and concentration dependent

The effects of MMP-7 on actin organization were directly related to the amount of MMP-7 activity added to hippo-campal cultures. We treated cultures with 1–100 mU/mL of MMP-7 for 1 h and found that the number of neurons responding to MMP-7 treatment with actin reorganization increased in a concentration-dependent manner (Fig. 5a). Half-maximal shifts occurred near 5 mU/mL (Fig. 5a). The spiny-to-rope morphological changes in actin were also time dependent, with an increase in the number of neurons with rope-like actin detectable within 10–20 min, and continuing up to 1 h (Fig. 5b).

MMP-7 effects are NMDA-R dependent

A rapid redistribution of F-actin from dendritic spines into dendritic shafts has previously been associated with NMDA receptor (NMDA-R)-mediated Ca^{2+} influx (Halpain *et al.* 1998; Hering and Sheng 2003). Indeed, cultures briefly treated with 50 μM NMDA for only 30 s showed similar F-actin rearrangements seen after MMP-7 treatment (Figs 6b and c). To test whether MMP-7-mediated F-actin rearrangements require Ca^{2+} influx through the NMDA-R, we blocked this channel with the specific antagonist MK-801 (10 μM). Strikingly, this antagonist completely abolished the effects of either NMDA application or MMP-7 treatment on F-actin organization in dendrites (Figs 6b and e). Quantitative analysis of cultures treated with MMP-7/MK-801 showed that the number of F-actin/synaptophysin double-positive puncta did not differ from control cultures treated with MK-801 alone (Fig. 6g). Average autocorrelation functions confirmed that MK-801 pretreatment completely prevented MMP-7 effects on F-actin reorganization (Fig. 6h). Western blotting of MMP-7-

treated cultures confirmed higher tyrosine phosphorylation on NR2A/B and showed that NMDA-R activation did not involve the proteolytic cleavage of NMDA-R subunits (supplemental material), and must therefore be an indirect effect. These results establish that MMP-7-induced rearrangements of F-actin are mediated by NMDA-R activation.

MMP-7 effects are substrate independent

Activated MMP-7 can cleave a variety of extracellular matrix proteins, including laminin and fibronectin (Wilson and Matrisian 1996). To determine if the observed effects were a result of MMP-7 cleavage of laminin, which was used as a substrate for the attachment and growth of hippocampal neuron cultures, MMP-7 effects were also tested in cultures grown on fibronectin or poly-DL-ornithine alone. After 15 DIV, there were no significant differences in the numbers of F-actin/synaptophysin double-positive puncta between cultures grown on the different substrates (Fig. 6a, Fig. 7a and d). MMP-7 effects on F-actin reorganization were also seen in cultures grown on fibronectin or poly-DL-ornithine alone (Figs 7b and e). Interestingly, cultures grown on poly-DL-ornithine, in the absence of laminin or fibronectin, showed a greater and irreversible response to MMP-7 (Fig. 7e). The number of F-actin clusters along the dendrites significantly decreased ($p < 0.001$) after MMP-7 treatment by 2.3 and 2.1 times in neurons cultured on laminin or fibronectin, respectively. Interestingly, the decrease was 10.3 times greater in cultures grown on poly-DL-ornithine alone (Fig. 6g, Figs 7c and f). Furthermore, a significant decrease in synaptophysin-positive puncta ($p < 0.001$) was seen with neurons cultured on poly-DL-ornithine after MMP-7 treatment (Fig. 7f). Moreover, pre-incubation with MK-801 (10 μM, 2 h) protected neurons from MMP-7 effects independently of substrate type (Fig. 6g, Figs 7c and f). As laminin and fibronectin are classic substrates for MMP-7, these results may reflect a dilution of MMP-7 activity in cultures that contained those substrates, resulting in higher MMP-7 activity in cultures lacking those substrates (i.e. poly-DL-ornithine only). As MMP-7 effects were stronger in cultures lacking laminin and fibronectin, the mechanism involved in opening NMDA-R does not require those substrates.

MMP-7-induced F-actin reorganization is reversible

Next, we examined whether MMP-7 effects on F-actin were reversible. Hippocampal cultures (15 DIV) were treated with MMP-7-containing medium for 1 h and then placed into normal conditioned medium with or without MK-801. The F-actin organization, synapse number, or cell survival, were analyzed after 2 h (Figs 8a–d). The F-actin changes induced by MMP-7 were reversible 2 h after withdrawal of MMP-7. The addition of MK-801 did not contribute to the recovery, indicating that MK-801 prevents, but does not reverse, MMP-7-induced changes. These results show that MMP-7 effects on F-actin are reversible.

Discussion

This report provides the first evidence that the stability of dendritic spine synapses can be disrupted by MMP-7. Using hippocampal neuron cultures, we have established that MMP-7 can transform mature spiny synapses into an immature, filopodial morphology. MMP-7 treatment resulted in a loss of spine-head F-actin staining that was accompanied by a dramatic accumulation of polymerized actin within dendritic shafts, giving a rope-like appearance. These cytoskeletal changes began within 10–20 min, indicating that a rapid mechanism is involved. Although the pathological significance of MMP-7 within the CNS is intriguing, these effects also reveal a mechanism that can profoundly affect dendritic spine morphology, and hence synaptic remodeling. MMP-7 cleavage of culture substrates was not a major factor in this mechanism as these responses occurred with neurons cultured on laminin, fibronectin or poly-DL-ornithine alone.

The morphological changes induced by MMP-7 were mediated by NMDA-R activation and completely blocked by the specific antagonist MK-801. It has also been reported that another protease, tissue plasminogen activator, can enhance NMDA-R activity through the proteolytic cleavage of NR-1, but it also requires the addition of exogenous NMDA-R agonists (Nicole *et al.* 2001; Fernandez-Monreal *et al.* 2004). MMP-7 is capable of cleaving fibrin, which is also a major substrate for plasmin activated by tissue plasminogen activator. However, we found that MMP-7 treatment does not increase the cleavage of NR-1, nor was the addition of exogenous glutamate required to induce the morphological changes. As dendritic spines are major postsynaptic sites of excitatory glutamatergic synapses, these MMP-7 effects either facilitate the presynaptic release of glutamate or enhance NMDA-R channel sensitivity, both of which are under further investigation.

Our findings suggest that MMP-7 effects in the CNS may run a spectrum from mild synaptic reorganization to triggering excitotoxicity. Modest levels of MMP-7, or perhaps other MMPs (Giuliani *et al.* 2005), could induce reversible remodeling of existing spines by disassembly of existing spines and extension of new filopodia, which would result in the creation of new synaptic contacts. Indeed, some studies have reported increased MMP-9 expression during dendritic remodeling after kainate-induced ischemic injury in the hippocampus (Szklarczyk *et al.* 2002). Interestingly, MMP-7 can process pro-MMP-9 into the fully active form. MMP inhibitors have been shown to block deafferentation-induced sprouting and synaptogenesis in rat dentate gyrus (Reeves *et al.* 2003). Therefore, pathological events that result in significantly high levels of MMP-7 within the brain may cause the loss of established connections, diminishing memories, associations or motor coordination. Such losses are common in traumatic CNS injuries and infections that disrupt the blood–brain barrier (Albensi and Janigro 2003; Witgen *et al.* 2005) and may lead to the excessive overstimulation of NMDA-R and excitotoxicity. Ischemic brain injuries are exacerbated by excitoxicity mediated by NMDA-R overstimulation, which has also been implicated as a precipitating factor for neuronal losses in Huntington's disease (Zeron *et al.* 2004), Alzheimer's disease and other neurodegenerative disorders (Lipton 2004). In an experimental autoimmune encephalomyelitis model for multiple sclerosis, we have also observed MMP-7 staining of infiltrating macrophages in perivascular cuffs, but not within parenchymal microglia (Douglas Ethell, unpublished observations). Therefore, local increases in MMP-7 levels within the CNS may lead to strong activation of NMDA-R and possibly excitotoxicity.

Although laminin and fibronectin substrates were not necessary, MMP cleavage of ECM components may still have contributed to these effects. For example, collagen cleavage by several MMPs, including MMP-7 (Lin *et al.* 2001), releases endostatin (NC1), a potent inhibitor of cell migration and angiogenesis that has also been shown to induce axonal outgrowth (Lein *et al.* 1991; Ackley *et al.* 2001). Interestingly, endostatin deposits have been reported in perivascular areas of Alzheimer's patient brains (Deininger *et al.* 2002). Although collagen is not widely expressed in the CNS, it is possible that some was co-purified from blood vessels during the preparation of neurons, or some collagen may have been released during the 15 days *in vitro*. Furthermore, the ability of MMPs to regulate integrin signaling is illustrated by the cleavage of laminin-5, which generates a γ2 fragment, exposing an otherwise inaccessible integrin-binding RGD site (Giannelli *et al.* 1997; Pirila *et al.* 2003). Similar mechanisms may alter spine morphology as well. Indeed, we have also observed that RGD-containing peptides can change spine morphology and actin organization in hippocampal neurons (Yang Shi and Iryna Ethell, in press), which are similar to the effects of MMP-7 and suggest that integrin signaling may play a role in the effects observed. Another major component of the ECM in the CNS is brevican, which is also cleaved by MMP-7 (Nakamura *et al.* 2000). Brevican is a member of the lectican family of chondroitin sulfate proteoglycans, which mediate the assembly of a peri-neuronal ECM

complex through interactions between their lectin domains and carbohydrates (Yamaguchi 2000). Moreover, MMP shedding of membrane cell adhesion protein cadherins can also affect the stability of synaptic contacts (Lochter *et al.* 1997; Noe *et al.* 2001; Takai *et al.* 2003). Whether MMP-7 cleavage of the ECM components or cell surface molecules contribute to its effects on spine morphogenesis are the subjects of future investigation.

In conclusion, the effects of MMP-7 on mature dendritic spine morphology and its known ability to cleave several proteins involved in the establishment of synaptic strength, lead us to suggest that the CNS effects of this metalloproteinase may be relevant to neurological disorders that compromise the blood–brain barrier and/or increase the infiltration of MMP-7 expressing cells.

Supplementary Material

Refer to Web version on PubMed Central for supplementary material.

Acknowledgments

Funding was provided by NIH grants AG21652 to DWE and MH67121 to IME, and Wellcome Trust (UK) to DAR.

Abbreviations used

ACF	autocorrelation function
DIV	days *in vitro*
ECM	extracellular matrix
GFP	green fluorescent protein
MMP	matrix metalloproteinase
MT-MMPs	membrane type-matrix metalloproteinases
NMDA-R	NMDA receptor
PBS	phosphate-buffered saline.

References

Ackley BD, Crew JR, Elamaa H, Pihlajaniemi T, Kuo CJ, Kramer JM. The NC1/endostatin domain of *Caenorhabditis elegans* type XVIII collagen affects cell migration and axon guidance. J. Cell Biol. 2001; 152:1219–1232. [PubMed: 11257122]

Albensi BC, Janigro D. Traumatic brain injury and its effects on synaptic plasticity. Brain Inj. 2003; 17:653–663. [PubMed: 12850950]

Anthony DC, Ferguson B, Matyzak MK, Miller KM, Esiri MM, Perry VH. Differential matrix metalloproteinase expression in cases of multiple sclerosis and stroke. Neuropathol. Appl. Neurobiol. 1997; 23:406–415. [PubMed: 9364466]

Cleary JP, Walsh DM, Hofmeister JJ, Shankar GM, Kuskowski MA, Selkoe DJ, Ashe KH. Natural oligomers of the amyloid-β protein specifically disrupt cognitive function. Nat. Neurosci. 2005; 8:79–84. [PubMed: 15608634]

Clements JM, Cossins JS, Wells GM, et al. Matrix metalloproteinase expression during experimental allergic encephalomyelitis and effects of a combined metalloproteinase and tumor necrosis factor-α inhibitor. J. Neuroimmunol. 1997; 74:85–94. [PubMed: 9119983]

Deininger MH, Fimmen BA, Thal DR, Schluesener HJ, Meyermann R. Aberrant neuronal and paracellular deposition of endostatin in brains of patients with Alzheimer's disease. J. Neurosci. 2002; 22:10 621–10 626. [PubMed: 11756483]

Dityatev A, Schachner M. Extracellular matrix molecules and synaptic plasticity. Nat. Rev. Neurosci. 2003; 4:456–468. [PubMed: 12778118]

Ethell DW, Buhler LA. Fas ligand-mediated apoptosis in degenerative disorders of the brain. J. Clin. Immunol. 2003; 5:363–370. [PubMed: 14601644]

Ethell IM, Pasquale EB. Molecular mechanisms of dendritic spine development and remodeling. Prog. Neurobiol. 2005; 75:161–205. [PubMed: 15882774]

Ethell IM, Yamaguchi Y. Cell surface heparan sulfate proteoglycan syndecan-2 induces the maturation of dendritic spines in rat hippocampal neurons. J. Cell Biol. 1999; 144:575–586. [PubMed: 9971750]

Ethell IM, Irie F, Kalo MS, Couchman JR, Pasquale EB, Yamaguchi Y. EphB/syndecan-2 signaling in dendritic spine morphogenesis. Neuron. 2001; 31:1001–1013. [PubMed: 11580899]

Ethell DW, Kinloch R, Green DR. Metalloproteinase shedding of Fas ligand regulates β-amyloid neurotoxicity. Curr. Biol. 2002; 12:1595–1600. [PubMed: 12372252]

Fernandez-Monreal M, Lopez-Atalaya JP, Benchenane K, et al. Arginine 260 of the amino-terminal domain of NR1 subunit is critical for tissue-type plasminogen activator-mediated enhancement of *N*-methyl-d-aspartate receptor signaling. J. Biol. Chem. 2004; 279:50 850–50 856.

Fiala JC, Allwardt B, Harris KM. Dendritic spines do not split during hippocampal LTP or maturation. Nat. Neurosci. 2002; 5:297–298. [PubMed: 11896399]

Furman C, Copin C, Kandoussi M, Davidson R, Moreau M, McTaggiart F, Chapman MJ, Fruchart JC, Rouis M. Rosuvastatin reduces MMP-7 secretion by human monocyte-derived macrophages: potential relevance to atherosclerotic plaque stability. Atherosclerosis. 2004; 174:93–98. [PubMed: 15135256]

Giannelli G, Falk-Marzillier J, Schiraldi O, Stetler-Stevenson WG, Quaranta V. Induction of cell migration by matrix metalloprotease-2 cleavage of laminin-5. Science. 1997; 277:225–228. [PubMed: 9211848]

Giuliani F, Fu SA, Metz LM, Yong VW. Effective combination of minocycline and interferon-β in a model of multiple sclerosis. J. Neuroimmunol. 2005; 165:83–91. [PubMed: 15958276]

Gjertsson I, Innocenti M, Matrisian LM, Tarkowski A. Metalloproteinase-7 contributes to joint destruction in Staphylococcus aureus induced arthritis. Microb. Pathog. 2005; 38:97–105. [PubMed: 15748811]

Halpain S, Hipolito A, Saffer L. Regulation of F-actin stability in dendritic spines by glutamate receptors and calcineurin. J. Neurosci. 1998; 18:9835–9844. [PubMed: 9822742]

Hartung HP, Kieseier BC. The role of matrix metalloproteinases in autoimmune damage to the central and peripheral nervous system. J. Neuroimmunol. 2000; 107:140–147. [PubMed: 10854648]

Hering H, Sheng M. Dendritic spines: structure, dynamics and regulation. Nat. Rev. Neurosci. 2001; 2:880–888. [PubMed: 11733795]

Hering H, Sheng M. Activity-dependent redistribution and essential role of cortactin in dendritic spine morphogenesis. J. Neurosci. 2003; 23:11 759–11 769.

Hughes PM, Wells GM, Perry VH, Brown MC, Miller KM. Comparison of matrix metalloproteinase expression during Wallerian degeneration in the central and peripheral nervous systems. Neuroscience. 2002; 113:273–287. [PubMed: 12127085]

Imai K, Hiramatsu A, Fukushima D, Pierschbacher MD, Okada Y. Degradation of decorin by matrix metalloproteinases: identification of the cleavage sites, kinetic analyses and transforming growth factor-β1 release. Biochem. J. 1997; 322:809–814. [PubMed: 9148753]

Kaufmann WE, Moser HW. Dendritic anomalies in disorders associated with mental retardation. Cereb. Cortex. 2000; 10:981–991. [PubMed: 11007549]

Kayed R, Head E, Thompson JL, McIntire TM, Milton SC, Cotman CW, Glabe CG. Common structure of soluble amyloid oligomers implies common mechanism of pathogenesis. Science. 2003; 300:486–489. [PubMed: 12702875]

Lein PJ, Higgins D, Turner DC, Flier LA, Terranova VP. The NC1 domain of type IV collagen promotes axonal growth in sympathetic neurons through interaction with the α1 β1 integrin. J. Cell Biol. 1991; 113:417–428. [PubMed: 2010469]

Lin HC, Chang JH, Jain S, Gabison EE, Kure T, Kato T, Fukai N, Azar DT. Matrilysin cleavage of corneal collagen type XVIII NC1 domain and generation of a 28-kDa fragment. Invest. Ophthalmol. Vis. Sci. 2001; 42:2517–2524. [PubMed: 11581192]

Lipton SA. Paradigm shift in NMDA receptor antagonist drug development: molecular mechanism of uncompetitive inhibition by memantine in the treatment of Alzheimer's disease and other neurologic disorders. J. Alzheimer's Dis. 2004; 6:S61–S74.

Lochter A, Galosy S, Muschler J, Freedman N, Werb Z, Bissell MJ. Matrix metalloproteinase stromelysin-1 triggers a cascade of molecular alterations that leads to stable epithelial-to-mesenchymal conversion and a pre-malignant phenotype in mammary epithelial cells. J. Cell Biol. 1997; 139:1861–1872. [PubMed: 9412478]

Lopez-Boado YS, Wilson CL, Hooper LV, Gordon JI, Hultgren SJ, Parks WC. Bacterial exposure induces and activates matrilysin in mucosal epithelial cells. J. Cell Biol. 2000; 148:1305–1315. [PubMed: 10725342]

Mitsiades N, Yu WH, Poulaki V, Tsokos M, Stamenkovic I. Matrix metalloproteinase-7-mediated cleavage of Fas ligand protects tumor cells from chemotherapeutic drug cytotoxicity. Cancer Res. 2001; 61:577–581. [PubMed: 11212252]

Mott JD, Werb Z. Regulation of matrix biology by matrix metalloproteinases. Curr. Opin. Cell Biol. 2004; 16:558–564. [PubMed: 15363807]

Nakamura H, Fujii Y, Inoki I, Sugimoto K, Tanzawa K, Matsuki H, Miura R, Yamaguchi Y, Okada Y. Brevican is degraded by matrix metalloproteinases and aggrecanase-1 (ADAMTS4) at different sites. J. Biol. Chem. 2000; 275:38 885–38 890.

Nicole O, Docagne F, Ali C, Margaill I, Carmeliet P, MacKenzie ET, Vivien D, Buisson A. The proteolytic activity of tissue-plasminogen activator enhances NMDA receptor-mediated signaling. Nat. Med. 2001; 7:59–64. [PubMed: 11135617]

Nimchinsky EA, Sabatini BL, Svoboda K. Structure and function of dentritic spines. Annu. Rev. Physiol. 2002; 64:313–353. [PubMed: 11826272]

Noe V, Fingleton B, Jacobs K, Crawford HC, Vermeulen S, Steelant W, Bruyneel E, Matrisian LM, Mareel M. Release of an invasion promoter E-cadherin fragment by matrilysin and stromelysin-1. J. Cell Sci. 2001; 114:111–118. [PubMed: 11112695]

Pirila E, Sharabi A, Salo T, Quaranta V, Tu H, Heljasvaara R, Koshikawa N, Sorsa T, Maisi P. Matrix metalloproteinases process the laminin-5 γ2-chain and regulate epithelial cell migration. Biochem. Biophys. Res. Commun. 2003; 303:1012–1017. [PubMed: 12684035]

Ramakers GJ. Rho proteins, mental retardation and the cellular basis of cognition. Trends Neurosci. 2002; 25:191–199. [PubMed: 11998687]

Reeves TM, Prins ML, Zhu J, Povlishock JT, Phillips LL. Matrix metalloproteinase inhibition alters functional and structural correlates of deafferentation-induced sprouting in the dentate gyrus. J. Neurosci. 2003; 23:10 182–10 189.

Rusakov DA, Kullmann DM, Stewart MG. Hippocampal synapses: do they talk to their neighbours? Trends Neurosci. 1999; 22:382–388. [PubMed: 10441295]

Szklarczyk A, Lapinska J, Rylski M, McKay RD, Kaczmarek L. Matrix metalloproteinase-9 undergoes expression and activation during dendritic remodeling in adult hippocampus. J. Neurosci. 2002; 22:920–930. [PubMed: 11826121]

Takai Y, Shimizu K, Ohtsuka T. The roles of cadherins and nectins in interneuronal synapse formation. Curr. Opin. Neurobiol. 2003; 13:520–526. [PubMed: 14630213]

Wilson CL, Matrisian LM. Matrilysin: an epithelial matrix metalloproteinase with potentially novel functions. Int. J. Biochem. Cell Biol. 1996; 28:123–136. [PubMed: 8729000]

Witgen BM, Lifshitz J, Smith ML, Schwarzbach E, Liang SL, Grady MS, Cohen AS. Regional hippocampal alteration associated with cognitive deficit following experimental brain injury: a systems, network and cellular evaluation. Neuroscience. 2005; 133:1–15. [PubMed: 15893627]

Woessner, F. Matrilysin. In: Barrett, AJ.; Rawlings, ND.; Woessner, F., editors. Handbook of Proteolytic Enzymes. 2nd edn. Vol. vol. 1. 2004. p. 532-538.

Yamaguchi Y. Lecticans: organizers of the brain extracellular matrix. Cell Mol. Life Sci. 2000; 57:276–289. [PubMed: 10766023]

Yong VW, Power C, Forsyth P, Edwards DR. Metalloproteinases in biology and pathology of the nervous system. Nat. Rev. Neurosci. 2001; 2:502–511. [PubMed: 11433375]

Yuste R, Bonhoeffer T. Morphological changes in dentritic spines associated with long-term synaptic plasticity. Annu. Rev. Neurosci. 2001; 24:1071–1089. [PubMed: 11520928]

Zeron MM, Fernandes HB, Krebs C, Shehadeh J, Wellington CL, Leavitt BR, Baimbridge KG, Hayden MR, Raymond LA. Potentiation of NMDA receptor-mediated excitotoxicity linked with intrinsic apoptotic pathway in YAC transgenic mouse model of Huntington's disease. Mol. Cell Neurosci. 2004; 25:469–479. [PubMed: 15033175]

Europe PMC Funders Author Manuscripts

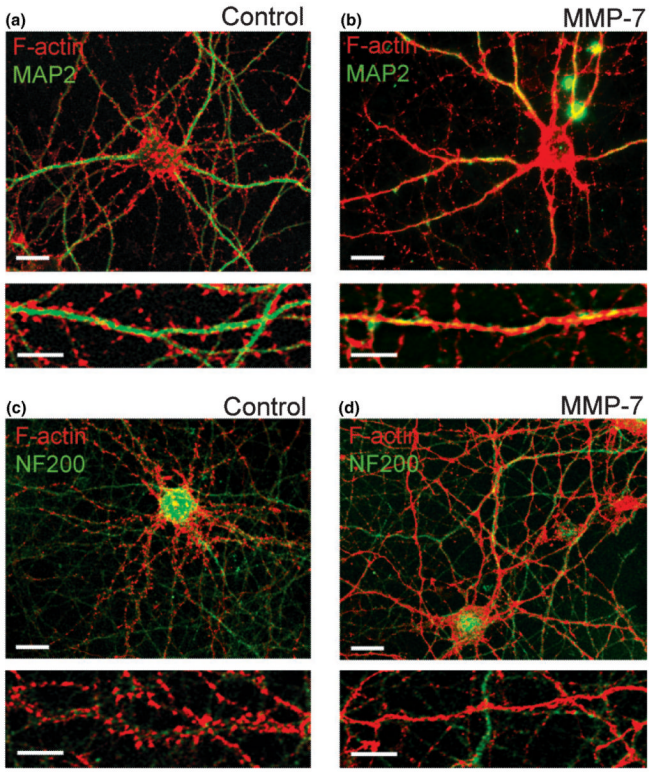

Fig. 1.

MMP-7 induces F-actin reorganization in dendrites of cultured hippocampal neurons. (a–d) Confocal images of control and MMP-7 treated hippocampal neurons at 15 DIV. F-actin polymerization was visualized by rhodamine-coupled phalloidin (red), dendrites by immunostaining for MAP2 (green; a, b), and axons by immunostaining for NF-200 (green; c, d). Scale bars: 10 μm (upper); 5 μm (lower).

Europe PMC Funders Author Manuscripts

Europe PMC Funders Author Manuscripts

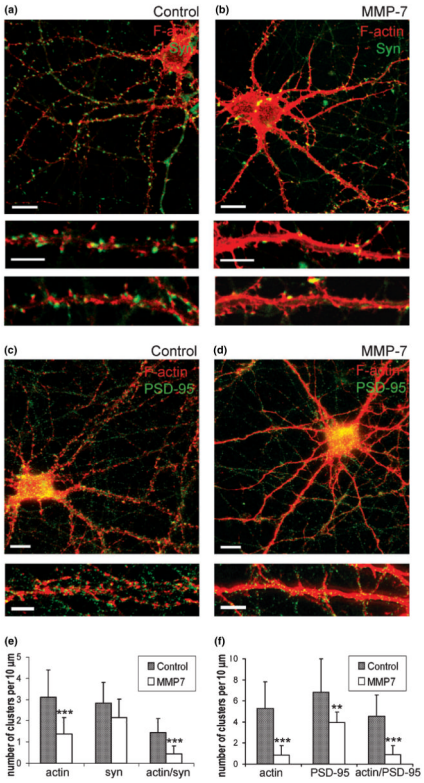

Fig. 2.

MMP-7 treatment induces F-actin rearrangement and reduces the number of PSD-95-positive postsynaptic sites and spiny synapses in cultured hippocampal neurons. (a–d) Confocal images of control and MMP-7 treated hippocampal neurons at 15 DIV. F-actin polymerization was visualized by rhodamine-coupled phalloidin (red), (a, b) presynaptic terminals by immunostaining for synaptophysin (green) and (c, d) postsynaptic sites by immuno-staining for PSD-95 (green). Scale bars: 10 μm (upper); 5 μm (lower). (e) Quantitative analysis of the number of F-actin, synaptophysin and actin/synaptophysin double-positive clusters per 10 μm of dendrite. (f) Quantitative analysis of the number of F-actin, PSD-95 and actin/PSD-95 double-positive clusters per 10 μm of dendrite. Vertical bars indicate SD; $n = 10$ neurons per group; $*p < 0.05$, $**p < 0.01$, $***p < 0.001$.

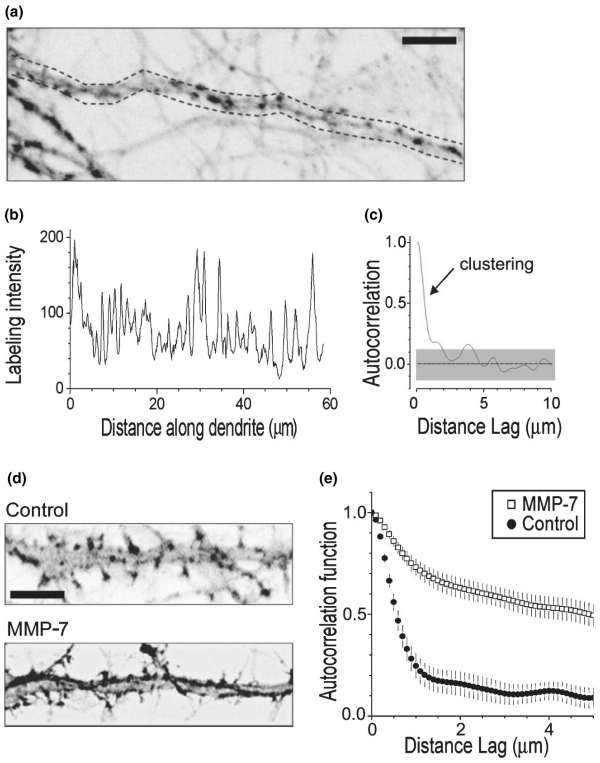

Fig. 3.

Quantitative evaluation of the F-actin labeling pattern in dendrites. (a) A dendritic fragment showing characteristic labeling for F-actin in baseline conditions. Image is superimposed with a sampling segment (dotted line) for labeling intensity reference. (b) The labeling intensity profile along the dendritic fragment in (a) shows average pixel values across the area within dotted lines. (c) Autocorrelation function (ACF) of the labeling profile shown in (b). Gray shaded area shows 95% confidence limits. The initial deflection indicates the presence of distinct, 1–2-μm wide spots/clusters of labeling. In comparison, random noise labeling would correspond to insignificant deviation of ACF from zero, whereas homogeneous labeling would tend to show ACF values close to unity. (d) Dendritic fragments showing characteristic labeling for F-actin in control and MMP-7 treated cultures. Scale bars: 5 μm (e). Average autocorrelation functions reflecting the labeling pattern of F-actin in dendrites in control cultures (Control, closed circles), and cultures incubated with MMP-7 (MMP-7, open squares); vertical bars, SEM ($n = 20$ dendrite fragments in each condition, see Fig. 1). The data indicate that the ~2-μm F-actin clusters, present in control conditions, are transformed into a more homogeneous type of labeling (statistical difference at lag distances above 1 μm is at least at $p < 0.05$; error bars, 95% confidence intervals).

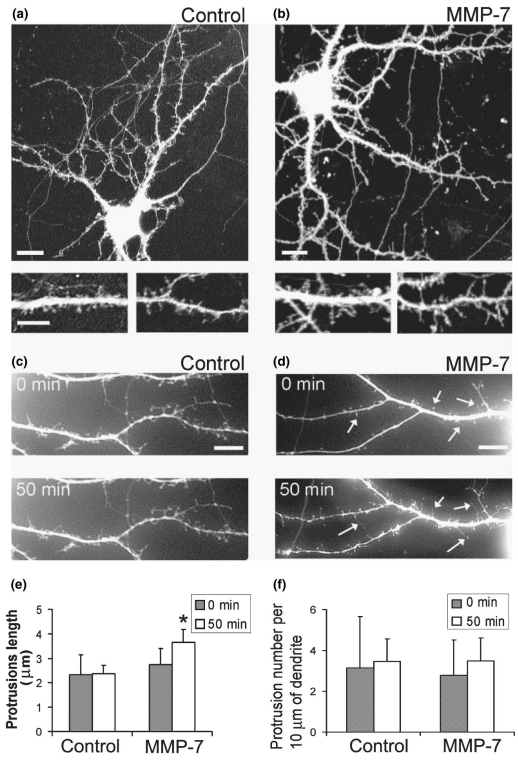

Fig. 4.

MMP-7 induces changes in dendritic spine morphology in 15-DIV hippocampal neuron cultures. (a, b) The confocal images of GFP-labeled hippocampal neurons from control and MMP-7 treated cultures. Scale bars: 10 μm (upper); 5 μm (lower). (c, d) Live images of GFP-labeled dendritic spines in 15-DIV hippocampal neurons before (0 min) and after (50 min) treatment with (c) control, or (d) MMP-7. MMP-7 treatment induced changes in dendritic spine morphology and promoted elongation of existing dendritic spines (arrows). Scale bars: 5 μm. (e) Quantification of dendritic protrusion length. (f) Quantification of dendritic protrusion density.

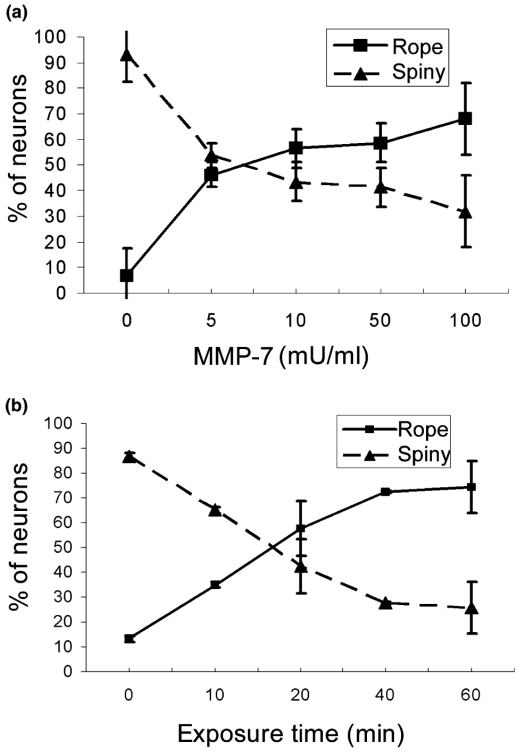

Fig. 5.

MMP-7 effects are time and concentration dependent in 15-DIV hippocampal neuron cultures. (a) Phalloidin-labeled dendrites were calculated for rope-like or spiny F-actin labeling after treatment with a series of MMP-7 concentrations for 1 h. The percentage of neurons showing rope-like dendrite labeling increased as more MMP-7 was added. (b) The percentage of neurons with rope-like F-actin labeling increased with time, in cultures treated with 100 mU/mL of MMP-7. Vertical bars indicate SD; $n = 1000$ neurons per group; $*p < 0.05$, $**p < 0.01$, $***p < 0.001$.

Europe PMC Funders Author Manuscripts

Europe PMC Funders Author Manuscripts

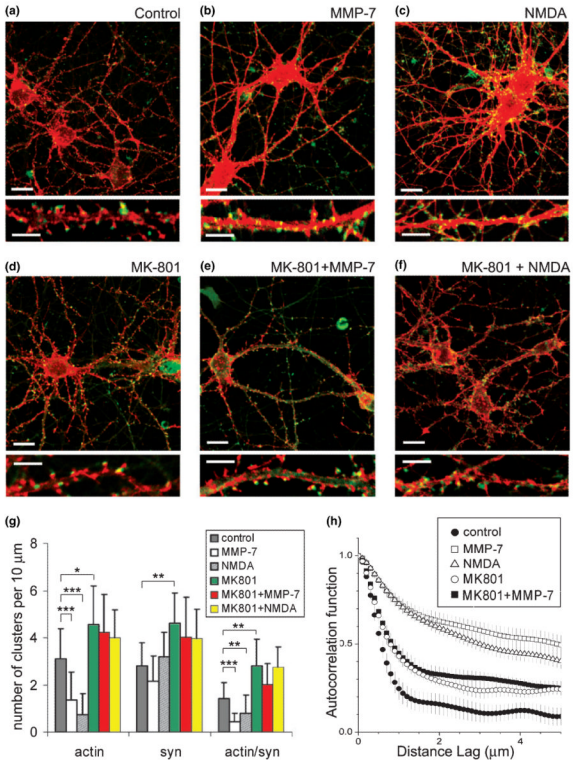

Fig. 6.

MMP-7 mimics NMDA effects and blockade of NMDA channels prevents MMP-7 mediated F-actin rearrangement. Confocal images of 15-DIV hippocampal neurons in (a) control cultures and cultures treated with (b) MMP-7, (c) NMDA, (d) MK-801, (e) MK-801 + MMP-7, and (f) MK-801 + NMDA. F-actin polymerization was visualized by rhodamine-coupled phalloidin (red), presynaptic terminals by immunostaining for synaptophysin (green). Scale bars: 10 μm (upper); 5 μm (lower). (g) Quantitative analysis of the number of F-actin, synaptophysin and actin/synaptophysin double-positive clusters per 10 μm of dendrite. Vertical bars indicate SD; $n = 10$ neurons per group; $*p < 0.05$, $**p < 0.01$, $***p < 0.001$. (h) Average autocorrelation functions reflecting the labeling pattern of F-actin along dendrites of cultured neurons in control and experimental conditions, as indicated; error bars, 95% confidence intervals.

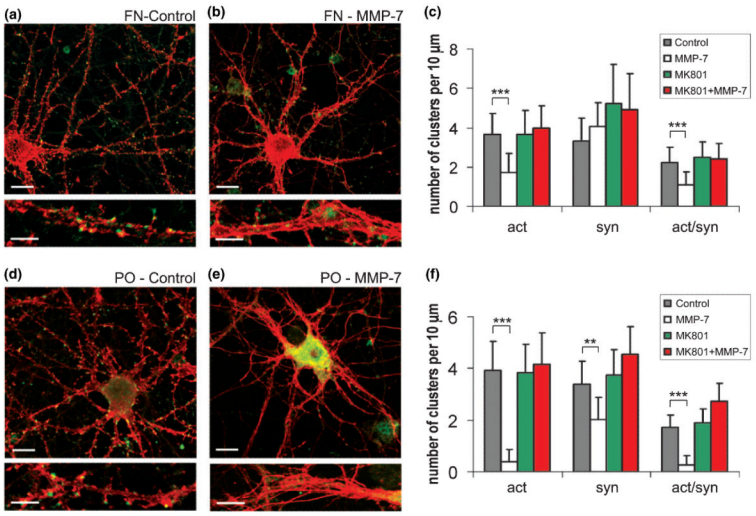

Fig. 7.

MMP-7 effects in cultures grown on fibronectin or poly-DL-ornithine alone. MMP-7 effects were compared in cultures grown on fibronectin or poly-DL-ornithine. Confocal images of 15-DIV hippocampal neurons in cultures grown on (a, b) fibronectin, and (d, e) poly-DL-ornithine alone. F-actin polymerization was visualized by rhodamine-coupled phalloidin (red), presynaptic terminals by immunostaining for synaptophysin (green). Scale bars: 10 μm (upper); 5 μm (lower). (c, f) Quantitative analysis of the number of F-actin, synaptophysin and actin/synaptophysin double-positive clusters per 10 μm of dendrite in cultures grown on (c) fibronectin, or (f) poly-DL-ornithine alone. Vertical bars indicate SD; n = 10 neurons per group; *$p < 0.05$, **$p < 0.01$, ***$p < 0.001$).

Europe PMC Funders Author Manuscripts

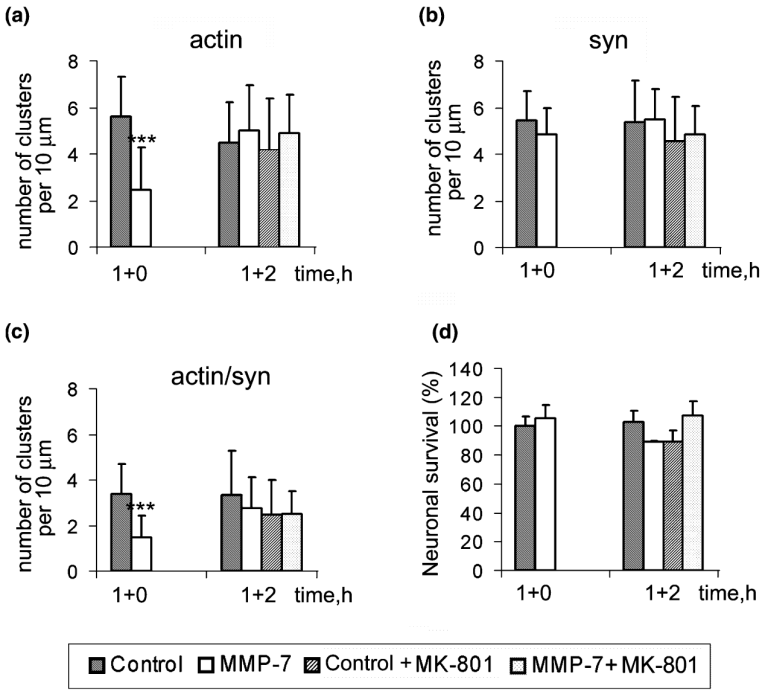

Fig. 8.

MMP-7-induced F-actin reorganization is reversible. Hippocampal neuron cultures (15 DIV) were treated for 1 h with control or MMP-7 containing medium (1 + 0), which was then replaced with normal or MK-801 containing medium for 2 h (1 + 2). (a–c) Quantitative analysis of the number of F-actin, synaptophysin and actin/ synaptophysin double-positive clusters per 10 µm of dendrite. (d) Quantitative analysis of neuronal survival.

Europe PMC Funders Author Manuscripts